



Feedforward weighted-samples based carrier frequency offset compensation in optical coherent M-QAM systems

Trung Hien Nguyen, Pascal Scalart, M Gay, L Bramerie, Christophe Peucheret, Michel Joindot

► To cite this version:

Trung Hien Nguyen, Pascal Scalart, M Gay, L Bramerie, Christophe Peucheret, et al.. Feedforward weighted-samples based carrier frequency offset compensation in optical coherent M-QAM systems. 43rd European Conference on Optical Communication (ECOC 2017), Sep 2017, Gothenburg, Sweden. pp.P1.SC3.40, 10.1109/ECOC.2017.8345923 . hal-01609730

HAL Id: hal-01609730

<https://hal.science/hal-01609730>

Submitted on 3 Oct 2017

HAL is a multi-disciplinary open access archive for the deposit and dissemination of scientific research documents, whether they are published or not. The documents may come from teaching and research institutions in France or abroad, or from public or private research centers.

L'archive ouverte pluridisciplinaire **HAL**, est destinée au dépôt et à la diffusion de documents scientifiques de niveau recherche, publiés ou non, émanant des établissements d'enseignement et de recherche français ou étrangers, des laboratoires publics ou privés.

Feedforward Weighted-Samples based Carrier Frequency Offset Compensation in Optical Coherent M-QAM Systems

T.-H. Nguyen⁽¹⁾, P. Scalart⁽²⁾, M. Gay⁽³⁾, L. Bramerie⁽³⁾, C. Peucheret⁽³⁾ and M. Joindot⁽³⁾

⁽¹⁾OPERA Department, Université Libre de Bruxelles, Brussels, Belgium, trung-hien.nguyen@ulb.ac.be

⁽²⁾INRIA/IRISA, University of Rennes 1, F-35000 Rennes, France

⁽³⁾FOTON Laboratory, CNRS, ENSSAT, University of Rennes 1, F-22305 Lannion, France

Abstract A low-complexity feedforward CFO compensation method is proposed and numerically validated for both square and cross M-QAM modulation in optical coherent systems. The proposed method is further compared to state-of-the-art methods and its effectiveness is experimentally verified in a 10-GBaud 16-QAM system.

Introduction

M-ary quadrature amplitude modulation (M-QAM) signals and coherent detection have become the key technologies for next-generation 400 Gbit/s per channel optical transmission systems¹. In the widely-used intradyne detection scheme, the carrier frequency offset (CFO) between the transmitter (Tx) and receiver (Rx) local oscillator lasers (LO) is compensated for in the digital domain in order to enable proper recovery of the signal. Extensive research on frequency offset estimation (FOE) has been carried out²⁻⁵. Among FOE methods, feedforward approaches are preferred to feedback implementations, since they tend to be more hardware-efficient⁴.

Time-domain (TD) FOE based on phase differentiation between 2 consecutive samples² or frequency-domain (FD) FOE based on periodograms obtained by fast-Fourier transforms (FFTs)³ are two major approaches. However, most of previous studies consider the two approaches separately. Fourth-power FOE (4thFOE) is widely used and applied mostly to square M-QAM constellations, e.g. 16-QAM. But its performance is degraded when cross M-QAM constellations, e.g. 32-QAM, are used and the number of samples employed for FOE is limited. FOE using the TD Viterbi-Viterbi monomial estimator (VVMFOE), has been recently reported and tested on 32-QAM constellations⁴. This method aims at assigning weight coefficients to symbols with different amplitude levels, usually by elevating with negative powers the amplitude of received samples for cross M-QAM signals. However, the use of negative power may make the hardware implementation more challenging. Recently, we have investigated a new FOE method based on the circular harmonic expansion (CHE) of the log-likelihood function (LLF) for both square and cross M-QAM signals⁵, called CHEFOE. However, the algorithm has only been numerically evaluated in the frequency domain.

In this paper, we investigate the CHEFOE

algorithm using both TD and FD approaches and compare its performance to that of the 4thFOE and VVMFOE methods. Compared to the negative power used in the VVMFOE method, the weight coefficients of symbols derived from the CHE can be easily implemented in a look-up table (LUT) providing a very hardware-efficient solution. Furthermore, we propose to weight samples in the coordinate rotation digital computer (CORDIC)-based polar coordinate system, leading to a multiplier-free weighted-samples implementation. We numerically investigate the performance of the proposed method for 16- and 32-QAM signals and experimentally validate its effectiveness with 16-QAM signals at 10 GBaud. To the best of our knowledge, the proposed CHEFOE is to date the most effective reported blind CFO compensation method for cross M-QAM signals in terms of complexity and successful estimation rate.

LLF expansion-based CFO estimator

At the receiver side (Rx), the samples of the received signal on one polarization at the symbol rate after perfect analog-to-digital conversion, timing recovery, linear and/or nonlinear compensation, can be represented as

$$r_k = s_k \exp(j2\pi k\phi_f + j\phi_{PN,k}) + n_k = x_k \exp(j\phi_k) \quad (1)$$

where $\{s_k\}$ are independent sequences of QAM symbols, n_k is the additive noise coming mainly from amplified spontaneous emission (ASE) that can be modeled as zero-mean complex additive white Gaussian noise (AWGN) with equal variances σ^2 for both real and imaginary parts. The terms $\phi_f = \Delta f T_S$ and ϕ_{PN} denote the normalized CFO and phase noise (PN), respectively, where T_S is the symbol period.

It is well known that 4thFOE can be used to estimate the CFO in quadrature phase-shift keying (QPSK or 4-QAM) systems². Its proper operation has been tested with square M-QAM signals³. The VVMPE method, an extension of CFO compensation working with cross M-QAM signals, has been proposed by elevating to the l -power the amplitude of the received samples x_k

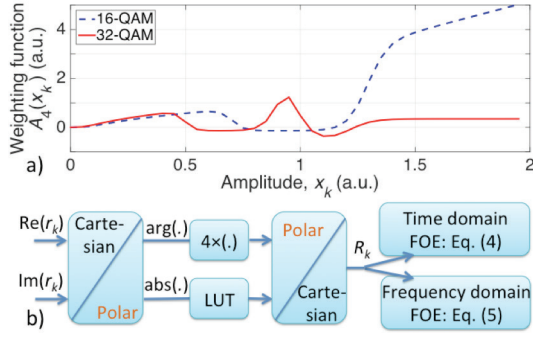


Fig. 1: a) Examples of CHEFOE weighting functions for 16- and 32-QAM. b) Efficient implementation of the CHEFOE with polar coordinates.

and to the 4^{th} -power the exponential term

$$R_k^{\text{VVM}} = (x_k)^l \exp(j4\phi_k) \quad (2)$$

where R_k is the nonlinear-transformed version of the received sample and the superscript VVM denotes the name of the FOE method. When $l = 4$, VVMFOE reduces to 4thFOE. The VVMFOE is optimized by exhaustively searching the suitable value of l that minimizes the considered performance metrics such as the bit-error-rate (BER) or the mean-square-error (MSE) of estimated CFO⁴. However, high and/or negative values of l result in a very high implementation complexity. The CHEFOE⁵ has recently been proposed as an efficient FOE solution with reduced complexity. Based on the Fourier series expansion along the phase ϕ of the LLF of the received samples, the first nonzero harmonic component of the LLF (fourth-harmonic) is retained to nonlinearly transform the amplitudes of the received samples

$$R_k^{\text{CHE}} = A_4(x_k) \exp(j4\phi_k) \quad (3)$$

where $A_4(x_k)$ is the fourth-harmonic weighting function of the sample amplitude x_k . It can be calculated beforehand according to⁶

$$A_4(x_k) = 1/\pi \int_0^{2\pi} F(0|x_k \exp(j\phi)) \exp(-j4\phi) d\phi,$$

where $F(0|x_k \exp(j\phi))$ is the probability density function of the received sample r_k . Examples of weighting functions for 16- and 32-QAM signals are shown in Fig. 1(a). By storing the weight value in a LUT, the power operation can be avoided, leading to a very efficient hardware implementation. We further use polar coordinates instead of Cartesian during the samples weighting, resulting in a multiplier-free implementation, as depicted in Fig. 1(b). This is made possible thanks to the fact that the term in four time $\arg(r_k)$ can be evaluated by a simple shifting operator⁷. It is obvious that the CHEFOE exhibits a lower complexity than the VVMFOE. Although the 4^{th} power operator in 4thFOE can also be implemented by the shift operator in polar coordinates, its performance is worse than the performance of CHEFOE, as will be shown later.

The weighted samples are then fed to either

TD or FD FOEs (Fig. 1(b)). The TD estimated CFO is obtained by calculating the mean phase increment over N samples

$$\hat{\phi}_f = 1/8\pi \cdot \arg \left(\sum_{k=2}^N R_k \cdot (R_{k-1})^* \right) \quad (4)$$

where $(\cdot)^*$ is the complex conjugate operator. The FD estimated CFO is achieved based on the maximization of the following periodogram

$$\hat{\phi}_f = 1/8\pi \cdot \arg \max_{\phi_f} \left| 1/N \sum_{k=1}^N R_k \exp(-j2\pi k\phi_f) \right|^2 \quad (5)$$

The periodogram can be computed efficiently by a N -FFT. Because of the 4^{th} power elevation of the phase component in Eq. (2)-(3), the estimated normalized CFO range lies within $[-1/8, 1/8]^3$. Note that the considered FD estimator can be cascaded with a fine step implementing a gradient-descent algorithm to fast converge and to minimize the MSE of the estimated CFO⁵.

Numerical investigation

We first numerically compare the performance of the FOE methods in a 10-GBaud 16- and 32-QAM coherent system. At the transmitting end, the M-QAM signals are generated by mapping a pseudo-random binary sequence (PRBS) with length of $2^{15}-1$ onto QAM constellations. About 130 000 QAM symbols are modulated onto the optical carrier and corrupted by AWGN noise during transmission. The noise is specified by the optical signal-to-noise ratio (OSNR in 0.1 nm) at the receiver input. The combined transmitter and LO laser PN is set to an equivalent linewidth of 100 kHz. To focus on the FOE function, other sources of impairments such as chromatic dispersion, polarization mode dispersion and timing clock recovery errors are assumed to be completely compensated for. At the receiver, the received symbols at the baud rate enter the FOE stage followed by PN compensation⁸. In all cases, the OSNRs at the receiver input are fixed at 18.2 dB and 20.9 dB (corresponding to an average BER of 3×10^{-4}) for 16- and 32-QAM signals, respectively. The normalized MSEs (NMSEs) of estimated CFO, defined as, $\mathbf{E}[\hat{\phi}_f - \phi_H^2]$ are calculated based on 500 runs of simulation. The optimized values of l in VVMFOE⁴ are equal to 9 and -2 for 16- and 32-QAM signals, respectively. Unless otherwise stated, the CFO is fixed to be 0.4 GHz in simulations and emulated to be the same value in the experiments. The block length (BL) is set to be 2^{11} .

Firstly, we investigate the impact of varying BL on the NMSE in Fig. 2. Considering FD FOEs, the performance of all algorithms is similar for 16-QAM when the block length is 2^8 . The required CHEFOE block length to achieve $\text{NMSE} < 10^{-7}$ for 32-QAM is 4 and 8 times smaller for CHEFOE than for VVMFOE and 4thFOE, respectively. With

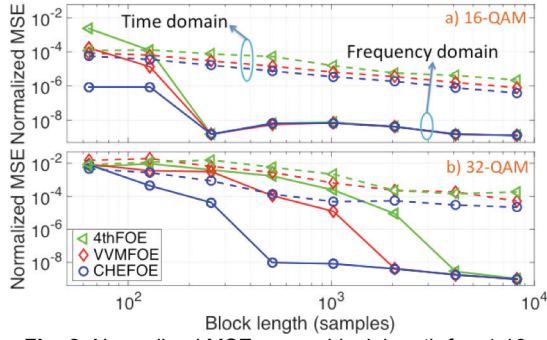


Fig. 2: Normalized MSE versus block length for a) 16-QAM, b) 32-QAM signals.

TD FOEs, CHEFOE always shows a better performance than the others methods. Note that FD methods can quickly estimate the CFO with a smaller number of required symbols compared to TD methods. Secondly, the successful estimation rate, defined as the ratio between the number of simulation runs resulting in acceptable CFO compensation (enabling to reach a BER $< 10^{-2}$) and the overall number of simulation runs, is plotted in Fig. 3. It is obvious that CHEFOE always provides a better successful estimation rate than the other methods, while presenting a lower complexity.

Experimental validation

In order to validate the principle of our proposed FOE and compare it with the other methods, a back-to-back single-polarization 10-Gbaud coherent system employing 16-QAM signals is used (Fig. 4(a)). The same laser with estimated linewidth of 100 kHz is used to modulate a 16-QAM signal at the Tx and as the LO at the Rx, thus allowing to introduce a precisely controlled and constant amount of CFO at the Rx. The OSNR is varied with the help of a variable attenuator placed before an optical amplifier (EDFA) and a 3-nm bandpass filter. At the Rx, signals are sampled at 40 GS/s. Different CFO values are then artificially introduced to the raw data, $r_k \leftarrow r_k \exp(j2\pi k \phi_f)$. Since the received samples exhibit inter-symbol interference (ISI) induced by the limited bandwidth of the signal generator at the Tx, a radius direct equalizer (RDE)⁹ is applied to remove the ISI. The received signal is then decimated to the symbol rate before being fed to the FOE and PN compensation⁸. Finally, the BER calculated with different FOEs is used for performance comparison.

The BER as a function of OSNR is presented in Fig. 4(b) for the different FOE methods in the time and frequency domains and for BL and CFO values of 2^{11} and 0.4 GHz, respectively. The BER

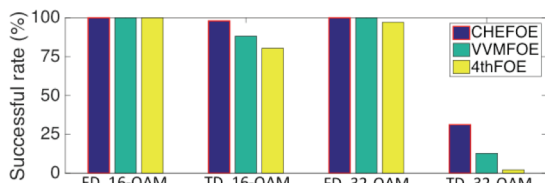


Fig. 3: Successful rate for different FOEs.

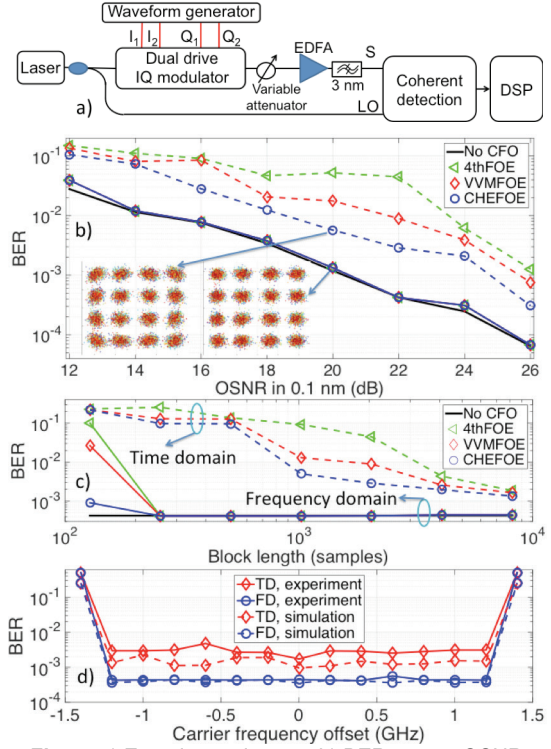


Fig. 4: a) Experimental setup. b) BER versus OSNR. c) BER versus block length at OSNR = 22 dB. d) BER versus different CFO values using CHEFOE method.

curve without CFO is also plotted as a benchmark. It can be seen that the FD FOE can effectively compensate for an emulated CFO regardless of the FOE method. Regarding TD FOEs, the CHEFOE outperforms the others. More specifically, at a BER of 10^{-3} , the OSNR penalty of CHEFOE is reduced by about 1 dB compared to that of VVMFOE and 4thFOE. The BER is further evaluated for different BL values at an OSNR of 22 dB (Fig. 4(c)). A BL of 2^8 is sufficient for FD FOEs to effectively compensate for the CFO, in agreement with the simulations, while TD FOE requires the BL to be larger than 2^{13} in order to minimize the OSNR penalty. Note that the TD CHEFOE always outperforms the other methods. Finally, we verify the effectiveness of CHEFOE for a wide CFO range (Fig. 4(d)). The CHEFOE operates properly in a CFO range of ± 1.2 GHz, and the experimental results agree with the numerical ones.

Conclusions

A weighted-sample based CFO compensation that can be efficiently implemented in either time- or frequency-domain is proposed. It has been numerically and experimentally validated. Compared to existing methods, it provides better performance and lower complexity.

References

- [1] P. J. Winzer, IEEE Commun. Mag., vol. 48, p. 26 (2010).
- [2] A. Leven et al., Photon. Technol. Lett., vol. 19, p. 366 (2007).
- [3] M. Selmi et al., Proc. ECOC, P3.08, Vienna (2009).
- [4] C. Spatharakis et al., Proc. CSNDSP, p.781, Manchester (2014).
- [5] T.-H. Nguyen et al., Proc. OECC, p. 1570100061, Shanghai (2015).
- [6] A. V. Petrov et al., Proc. ICC, p. 4756, Budapest (2013).
- [7] M. Rupp et al., Proc. Globecom, p. 6, San Francisco (2000).
- [8] T.-H. Nguyen et al., Proc. OFC, Tu3K.3, Anaheim (2016).
- [9] I. Fatadin et al., J. Lightw. Technol., vol. 27, p. 3042 (2009).